25 Solomon, D. H. and Rossar, M. J. *J. Appl. Polym. Sci.* 1965, **9**, 1261
26 Matsumoto, T., Sakai, I. and Arihara, M. *Kobunshi Kagaku* 1969, **26**, 378
27 Nakatsuka, T., Kawasaki, H. and Itadani, K. *Bull. Chem. Soc. Jpn.* 1977, **50**, 2829
28 Higashimura, T. and Nishii, H. *J. Polym. Sci.-Polym. Chem. Edn.* 1977, **15**, 329
29 Higashimura, T. *J. Polym. Sci.-Polym. Symp.* 1976, **56**, 71
30 Hiza, M., Hasegawa, H. and Higashimura, T. *Polym. J.* 1980, **12**, 379
31 Hamaya, T. and Yamada, S. *Makromol. Chem.* 1979, **180**, 2979
32 Hamaya, T. and Yamada, S. *Makromol. Chem. Rapid Comm.* 1980, **1**, 379
33 Imai, K. *PhD Thesis* Kyoto University 1965

Eutectic crystallization of poly(L-lactic acid) and pentaerythrityl tetrabromide

R. Vasanthakumari
Department of Inorganic and Physical Chemistry, Indian Institute of Science, Bangalore-560 012, India
(*Received* 7 *July* 1980; *revised* 12 *November* 1980)

Introduction

Diluents (either low molecular weight compounds or other polymers) are known to modify the morphology, the rates of nucleation and growth of polymers[1-4]. Recently binary systems in which both the components crystallize simultaneously to give a eutectic solid have been studied with great interest. Carbonnel *et al.*[5] have studied binary systems containing polyester and a variety of low molecular weight crystalline diluents and recently crystallization and melting behaviour of polyoxymethylene and glutaric acid has been reported[6]. Smith and Pennings[7,8] have studied the morphology resulting from the eutectic crystallization of polyethylene and a number of diluents and the porous microstructure that remains after the removal of the low molecular weight diluent from the solidified eutectics.

It has been shown[9] that poly(L-lactic acid) of molecular weight $M_v = 1.5 \times 10^5$ forms a eutectic with the dendritic growing diluent, penetaerythrityl tetrabromide, the eutectic composition being 46% by weight of the polymer at the eutectic temperature of 422K and the removal of the diluent from the solidified eutectic produces porous material. Here the studies have been extended to determine the influence of molecular weight of the polymer on the eutectic forming system consisting of poly(L-lactic acid), PLLA and pentaerythrityl tetrabromide. Extensive work has been carried out on crystallization kinetics of homopolymers and copolymers whereas no work has been reported on the crystallization kinetics of eutectic mixtures. Thus the present work is concerned with (i) the systematic study of the influence of molecular weight on the eutectic system PLLA-pentaerythrityl tetrabromide (ii) the kinetics of isothermal crystallization of a eutectic mixture at different temperatures since this will provide information about the mechanism underlying the eutectic crystallization process.

Experimental

Samples of different molecular weight were obtained by cationic ring-opening polymerization[10] of (L-) dilactide (supplied by Boehringer and Sions, Ingelheim, Germany) using a catalyst, stannous octoate. The samples were stored over phosphorus pentoxide. Viscosity average molecular weight (M_v) was determined in chloroform at 25°C with an Ubbelohde viscometer using the relation[10]: $[\eta] = 5.45 \times 10^{-4} M_v^{0.73}$. The solvent employed for the eutectic crystallization of PLLA was pure pentaerythrityl tetrabromide. The polymer solutions (about 5 mg) of different compositions were heated 20°C above their melting points in sealed aluminium pans, kept for 30 min for homogenizing, quenched fast to 100°C and then scanned at the rate of 8°C min^{-1} using a Perkin Elmer DSC IB in order to obtain the melting thermograms. Similar experiments were carried out for PLLA samples of different molecular weight. Calibration of d.s.c. has been carried out using standard samples with melting point in the measured range of temperature.

PLLA used for eutectic crystallization kinetics study had molecular weight $M_v = 1.8 \times 10^5$. The eutectic samples (46% by weight of PLLA) of about 5 mg were heated 30°C above the melting point, cooled fast to the respective crystallization temperature and rates of isothermal crystallization were folltowed using the Perkin Elmer DSC IB with a high chart speed of 160 mm min^{-1}.

Results and Discussion

As PLLA was prepared by cationic ring-opening polymerization, it contained a relatively small molecular weight distribution[10]. The thermal behaviour of the PLLA-pentaerythrityl tetrabromide mixtures was investigated by means of differential scanning calorimeter and the melting point-composition phase diagram of the above system was drawn for PLLA samples of different molecular weight. The melting points obtained for all the eutectic samples are not true equilibrium melting points but they correspond to that at the crystallization temperature, 100°C. The corresponding values of eutectic composition, C_E and eutectic temperature, T_E were determined from the phase diagrams. *Table 1* gives eutectic com-

Table 1 Values of eutectic composition and eutectic temperature for PLLA of different molecular weight

$[\eta]$	$M_V \times 10^{-5}$	C_E wt % of polymer at eutectic point	T_E (K) Eutectic temperature
1.85	0.68	50.00	421
2.45	1.00	49.34	421
3.3	1.50	46.0	422
3.8	1.80	46.1	422
4.9	2.60	45.45	422
6.1	3.5	45.21	423

0032-3861/81/070862-04$02.00

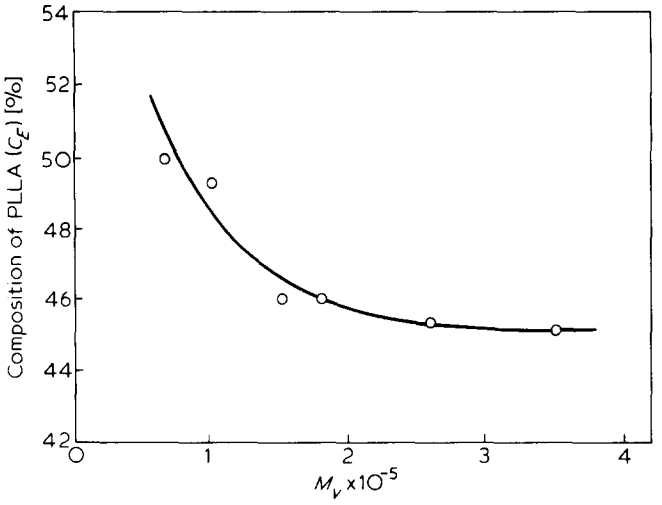

Figure 1 Composition of PLLA at the eutectic point, C_E as a function of molecular weight of PLLA

positions and the eutectic temperatures of PLLA of different molecular weights. The influence of molecular weight (M_v) of the polymer on the eutectic composition is presented in *Figure 1*. As the molecular weight increases the composition of the polymer in the eutectic decreases. The reason could be that the mutual diffusion of polymer segments and solvent molecules is the most pertinent requirement for the simultaneous crystallization process of the phases from the liquid phase to occur in a cooperative manner. It is known that the rate of diffusion of macromolecules strongly depends on molecular weight i.e. the viscosity of the melt increases with the increase of molecular weight as a result of which, transport of molecules into the surface becomes difficult. Furthermore the entanglement structure present in concentrated solutions of high molecular weight prevents the eutectic solidification. Hence it is quite understandable to find (*Figure 1*) that the eutectic composition contains a higher percentage of PLLA as the molecular weight of PLLA is reduced and *vice versa*.

Figure 2 depicts the relation between molecular weight of PLLA and eutectic temperature and it is clear that there is no appreciable change in the value of eutectic temperature as the molecular weight was changed. The data clearly shows that the eutectic composition is greatly affected by the molecular weight of the polymer whereas eutectic temperature remains unaffected. Similar behaviour has been observed[11] in the case of polyethylene—1, 2, 4, 5 tetrachlorobenzene eutectic system. Thus the molecular weight effects in this eutectic system are considered to be diffusion effects and the nucleation terms are not involved because the molecular weight dependence is reciprocal to eutectic composition (*Figure 1*) and the eutectic point is almost invarient with molecular weight (*Figure 2*).

In order to understand the mechanism of the eutectic crystallization process a study has been undertaken to determine the kinetics of isothermal crystallization of the eutectic mixture. The PLLA used in this study had a molecular weight of $M_v = 1.8 \times 10^5$. The eutectic samples were melted at temperatures 30°C above the eutectic melting point and rapidly cooled to the required isothermal crystallization temperature. Crystallization rate was followed using differential scanning calorimeter. The induction period for the crystallization was sufficiently long (for example 4 min at 388K) so that the isothermal temperature was maintained before the start of crystallization. Since the eutectic crystallization rate was relatively high compared with pure PLLA, the range and recorder chart speed were selected so as to yield reasonably large exotherms for accuracy in data analysis. The exothermic crystallization reaction was considered to be complete when the recorder pen levelled off to the initial base line.

Isothermal crystallization experiments were carried out in the temperature range 388–403K. Quantitative kinetic data could be obtained in the temperature range 388 to 403K from the corresponding exotherms by measuring the areas under the exothermic peak. When a_t and a_∞ are the areas under the exothermic peak at time, t and at the end of crystallization respectively, the Avrami equation is given by

$$\frac{a_\infty - a_t}{a_\infty} = e^{-kt^n}$$

where k is the rate donstant and n is the Avrami exponent.

Crystallization rate isotherms obtained for different temperatures are shown in *Figure 3* where $\frac{a_\infty - a_t}{a_\infty}$, the fraction of the amorphous material is plotted against log t. The values of k and n could be obtained by plotting

$$\log\left[-\log\frac{a_\infty - a_t}{a_\infty}\right]$$

against the logarithm of time (*Figure 4*). A linear relation is obtained in the first part of the transformation with slope equal to ~ 2. From *Figure 5* it is clear that eutectic crystallization is complicated because two stage crystallization has taken place and a break occurs in the plot. That is, after the primary crystallization has passed over a particular point at time r, a second crystallization step has started at a lower rate also following an Avrami type expression with a lower value of Avrami exponent ($n_2 < 1$). *Table 2* gives the various values of the Avrami exponents n_1 and n_2 and the corresponding k_1 and k_2 values obtained by using a computer program from the Avrami equation at different crystalliztion temperatures. The experimental values of n_1 and n_2 are not whole numbers but are fractional and furthermore n_2 is less than n_1. In the literature there are many cases in which polymers are shown to exhibit fractional values of

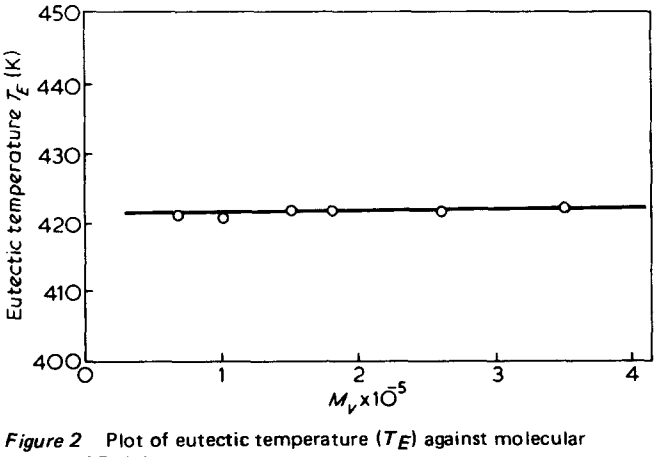

Figure 2 Plot of eutectic temperature (T_E) against molecular weight of PLLA

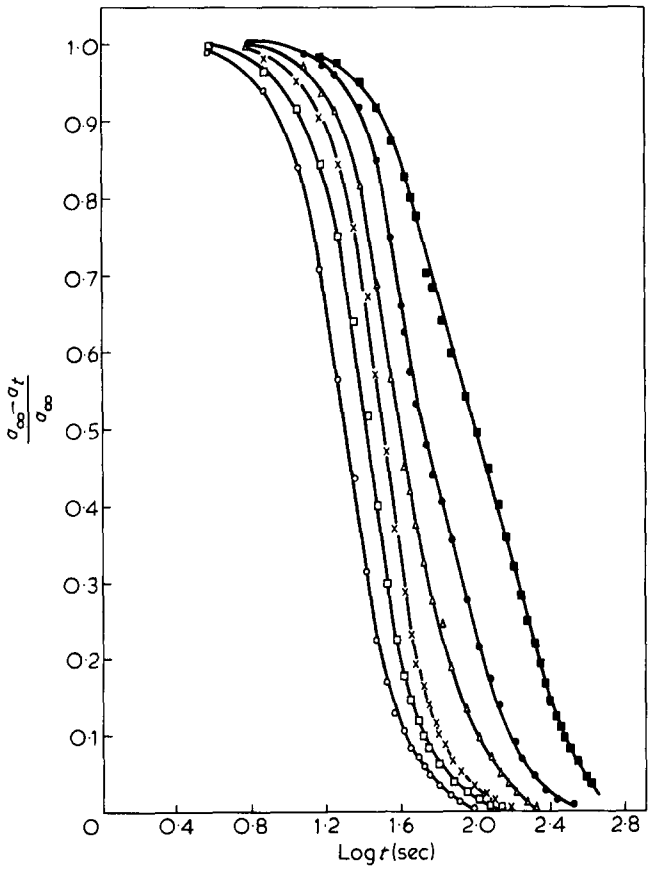

Figure 3 Plot of $a_\infty - a_t/a_\infty$ against log t for eutectic crystallization of the system PLLA – pentaerythrityl tetrabromide at indicated temperatures. (○), 388K; (□), 390K; (x), 392K; (△), 397K; (●), 400K; (■), 403K

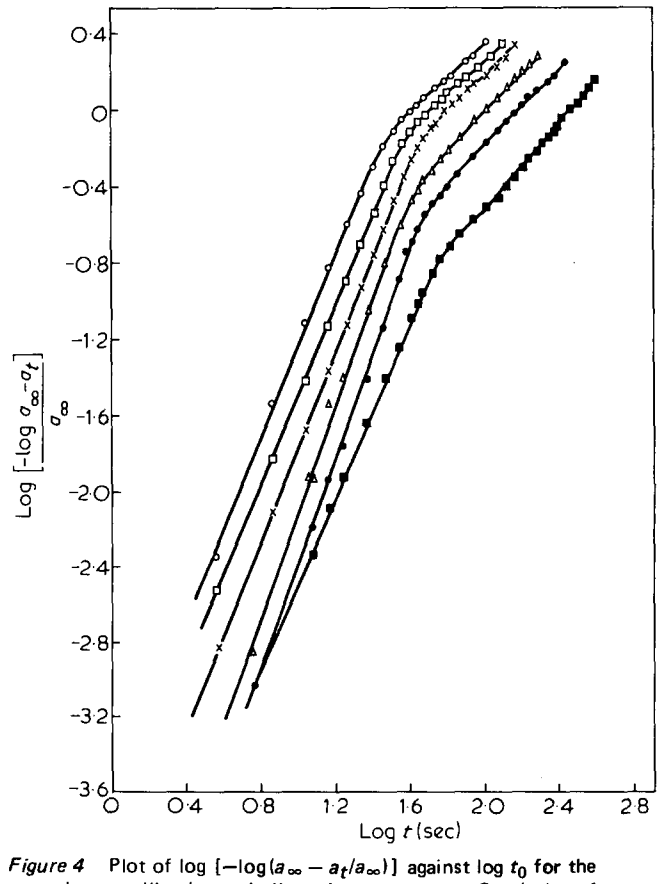

Figure 4 Plot of log $[-\log(a_\infty - a_t/a_\infty)]$ against log t_0 for the eutectic crystallization at indicated temperatures. Symbols as for *Figure 3*

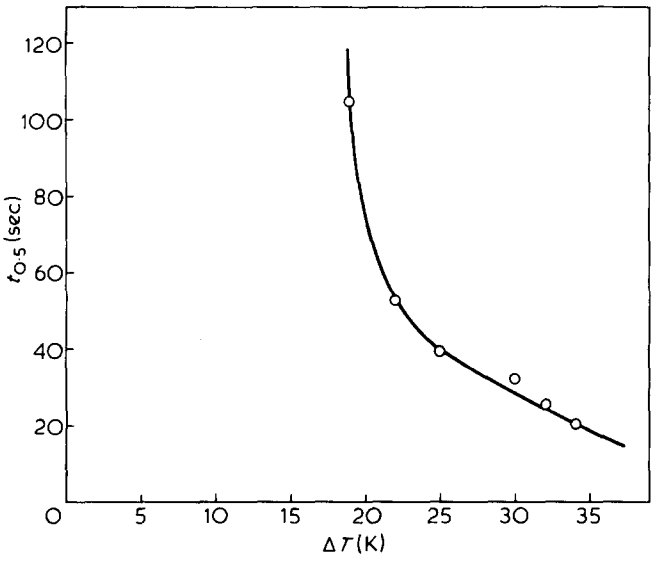

Figure 5 Crystallization half times ($t_{0.5}$) as a function of undercooling (ΔT)

Table 2 Kinetic data on eutectic crystallization

T_c (K)	n_1	k_1 sec^{-1}	n_2	k_2 sec^{-1}
388	2.3	0.0002438	0.88	0.036
390	2.3	0.0001374	0.86	0.033
392	2.4	0.0000601	0.86	0.027
397	2.5	0.00004027	1.04	0.0078
400	2.6	0.0000106	1.04	0.0050
403	2.2	0.0000126	1.1	0.00166

Avrami exponent [12–16]. Further two stage crystallization as a compensation of overall crystallization rate has been explained clearly by Hillier[17], Hoshino *et al.*[18], Keith[19] and Peterlin[20].

Crystallization half times ($t_{0.5}$) obtained are plotted against ΔT, the extent of supercooling in *Figure 5* where $\Delta T = T_m - T$, T_m is the eutectic melting point and T, the crystallization temperature.

Direct microscopic experiments revealed that the simultaneous crystallization of the polymer and the diluent proceeded in such a way that the diluent rods were the leading phase. Further it has been shown[9] that the PLLA microstructures (in the growth direction) left behind after sublimation of the solvent under reduced pressure from eutectic solution revealed long pores with a tendency to line up in the growth direction which is originated from the diluent rod-like crystals. The Avrami exponent obtained for the eutectic system (*Table 2*) confirms the above observation i.e. the solvent rods are the initiating phase. A schematic model has been suggested for the eutectic crystallization of the system poly propylene-pentaerythrityl tetrabromide[21]. Similarly the rod like eutectic structure has been observed in this system also.

Acknowledgement

The author is greatly indebted to Prof. A. J. Pennings and B. Eling, State University of Groningen, Netherlands, for supplying the samples and the discussions she had with them.

References

1 Keith, D. H. and Padden, F. J. *J. Appl. Phys.* 1964, **35(4)**, 1270
2 Nishi, T. and Hang, T. T. *Macromolecules* 1975, **8**, (6), 909
3 Boon, J. and Azene, J. M. *J. Polym. Sci. A-2* 1968, **6**, 885
4 Geil, P. 'Polymer single crystals', Wiley Interscience, New York, 1963
5 Carbonnel, L., Rosso, J. C. and Guieu R. *et al., Bull. Soc. Chim., France* 1970, **8–9**, 2849–2855; 1972, **3**, 934; 1973, **9 10**, 2776–2780
6 Gryte, C. C., Berghmans and Smets, *J. Polym. Sci. Polym. Phys. Edn.* 1979, **17**, 1295–1305
7 Smith, P. and Pennings, A. J. *Polymer* 1974, **15**, 413
8 Smith, P. and Pennings, A. J. *J. Polym. Sci. Polym. Phys. Edn.* 1977, **15**, 523–540
9 Vasanthakumari, R. and Pennings A. J. to be published
10 Schindler, A. and Harper, D. *J. Polym. Sci. Chem. Edn.* in press
11 Zamora, F. D. *Thesis*, Facultad de Ciencias Quimicas de San de San Sebastian, Spain
12 Hatano, M. and Kambara, S. *Polymer* 1961, **2**, 1
13 Sharples, A. and Swinton, F. L. *Polymer* 1963, **4**, 119
14 Banks, W., Gordon, M., Roe, R. J. and Sharples, A. *Polymer* 1963, **4**, 61
15 Gordon, M. and Hillier, I. H. *Trans Faraday Soc.* 1964, **60**, 763
16 Banks, W. and Sharples, A. *Macromol. Chem.* 1963, **59**, 233
17 Hillier, I. H. *J. Polym. Sci. 1965*, **A 3**, 3067
18 Hoshino, S., Meinecke, E., Powers, J., Stein, R. S. and Newman, S. *J. Polym. Sci. 1965*, **A-3**, 3041
19 Keith, I. D. *Kolloid Z.Z. Polym.* 1969, 231, 428
20 Peterlin, A. *J. Appl. Phys. 1964*, **35**, 80
21 Smith, P. *Thesis*, State University of Groningen, Groningen

Electron induced (surface) conductivity of FEP

J. P. Jog, S. J. Walzade and S. V. Bhoraskar
Department of Physics, University of Poona, Poona 411 007, *India*
(*Received* 27 *October* 1980; *revised* 24 *February* 1981)

Introduction

The incidence of electrons on an insulating material generates electron-hole pairs within the lattice and under the influence of an applied electric field the passage of charge carriers from one electrode to another constitutes a conduction current. This is the phenomenon of electron beam induced conduction and can be classified into *EBIC* (Bulk) and *EBIC* (Surface). The former is identified when the electric field is applied across the thickness of the sample and the latter when the electric field is applied parallel to the surface. *EBIC* (Bulk) is often used to study the diffusion lengths[1] and mean life time[2] of the charge carriers in semiconductors. The mobilities and transit times for holes and electrons have been determined[3,4] using the *EBIC* (Bulk), while Blumtrill[5] *et al.* have utilized this to investigate the dislocations in semiconductors.

Although an extensive work has been reported in the field of *EBIC* (Bulk) in oxides[6,7] and polymers[8–10], the *EBIC* (Surface) has not been studied in the literarure. In this communication we report the *EBIC* (Surface) in the copolymer: Fluorinated Ethylene-Propylene (FEP) as a function of incident electron flux and electron beam energy. The electric field in the measurement is applied parallel to the surface and the change in the conductivity due to the incidence of electrons near the field region is noticed. An attempt has been made to determine the spatial depth of trapping levels in FEP using the *EBIC* (surface).

Experimental

The experiments were performed on 250 μm thick films of fluorinated ethylene-propylene (11%–18% HFP in PTFE Du Pont de Nemours) at pressures less than 10^{-6} torr using an electron beam from an electron gun and accelerating column. Two concentric annular electrodes of silver with radial width of 1 mm each were vacuum deposited on one of the surfaces of the sample. The radial separation between the two rings and the inner diameter of the inner electrode were 2 mm each. A bias voltage was applied across the two electrodes making the outer electrode positive with respect to the inner electrode and a focussed beam of 1 mm diameter was allowed to fall at the centre of the annular electrodes, region *X*. A conical cage was mounted so as to establish contact with the inner electrode and to avoid any stray electrons from reaching the outer electrode directly. The current was recorded on the outer electrode using an electrometer amplifier. The beam energy was varied from 6 KeV to 30 KeV and the beam current was varied from 2×10^{-9} Amp to 2×10^{-8} Amp. The electron beam induced current I_s was recorded for the bias voltages ranging from 0 to 1000 V. The incident beam current I_p was measured on the conical cage when the beam was deflected using the beam scanning assembly. The experimental setup is shown in *Figure 1*.

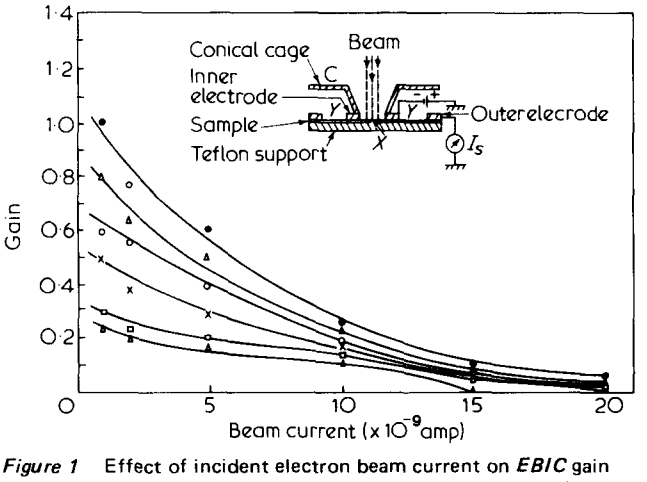

Figure 1 Effect of incident electron beam current on *EBIC* gain at constant beam energy for different biasing voltages and schematic diagram of experimental assembly. (●), 1000V; (▲), 900V; (○), 700V; (X), 500V; (□), 400V; (△), 300V: beam energy = 6KeV

0032 3861/81/070865-03$02.00